

Power management analysis for V2G (Vehicle-to-Grid) applications in a microgrid with photovoltaic source

Z. A. Padhya¹, S. S. Bohra^{1,*}

¹ Department of Electrical Engineering, Sarvajani College of Engineering & Technology, Surat, Gujarat, India

Received: 16 September 2020; Revised: 17 November 2020; Accepted: 11 December 2020; Published: 30 December 2020

Turk J Electrom Energ Vol.: 5 No: 2 Page: 61-73 (2020)

SLOI: <http://www.sloi.org/>

*Correspondence E-mail: shabbir.bohra@scet.ac.in

ABSTRACT The impact of the irregularity of the in-feed electricity on the power supply networks must be met with new concepts and technologies, such as peak shaving and reactive power management, *etc.* These actions facilitate also limiting carbon emission and associated footprints. This study aimed to investigate how a microgrid can support further enlargement of renewable energy source (RES) based plants as a collaborating unit in the power supply network. The microgrid consists of conventional and/or renewable energy sources, like solar energy, wind energy, bio-gas based, *etc.* Among these, the PV system is one of the most appreciated RESs being abundant and inexhaustible. In this study, analysis for grid-connected PV systems has been carried out to reveal the effects of electric vehicle (EV), which represents a mobile battery energy storage system (BESS). The EV could be treated as the best energy storage device under a scenario where a large number of EVs are deployed. The additional storage could not be required as the electric vehicles' batteries themselves act as a reasonable source of energy. The fleet of EVs will ensure minimum stress on the power grid under the vehicle-to-grid (V2G) concept. The EV batteries can be charged either from the utility grid during the off-peak period or through solar PV during day-time; and during peak load hours, the same batteries can be allowed to discharge into the grid to meet peak demands. Hence, the stability of the grid can be improved by implementing the V2G concept. The simulation results show the nature of power flow in the microgrid for various operating modes implemented on the MATLAB[®]/Simulink platform. This study helps in planning and power management of solar PV dominating microgrid catering fleet of EVs.

Keywords: Renewable energy source, V2G (vehicle-to-grid), Photovoltaic, Battery energy storage, Maximum power point tracking, Plug-in electric vehicle, Instantaneous symmetrical component theory

Cite this article: Z. A. Padhya, S. S. Bohra, Power management analysis for (Vehicle-to-Grid) V2G applications in a microgrid with photovoltaic source, Turkish Journal of Electromechanics & Energy, 5(2), 61-73, (2020).

1. INTRODUCTION

Adverse effects of pollution due to unlimited use of fossil fuels especially in the transportation sector and electric power generation industry have become alarming. Therefore, the rapidly increasing use of fossil fuels gives a wake-up call for finding substitute energy sources for these domains. The future of the oil economy is considered to be highly dependent on vehicle fleets in the world. It is not only temporary but also increasing with technological advancement. Besides, the burning of fossil fuels produces greenhouse gases (GHG), which highly affect world climate. On the other hand, electric vehicles (EVs) are among the promising solutions [1]. The EV helps the world reduce GHG emissions and fossil fuel utilization. Also, the development of EVs was step

up due to rising oil and gas prices, and advancement in battery technology [2].

Power demands will expand gradually because of the popular choice to take up Plug-in electric vehicles (PEVs) in the world and the rising population. It has become a challenge for discovering and managing additional power resources for ever-increasing demands. Renewable energy sources play an important role in this challenge. However, an energy storage system (ESS) should be employed to facilitate and control renewable energy resources. Furthermore, the PEV battery can be used as an ESS to store energy at a definite time and use it at another time in the transportation system [3]. Such flexibility can only be feasible where several energy sources with different

characteristics are participating. Moreover, the system is comprising of diversified loads such as a blend of linear, non-linear, active, and reactive kinds.

A microgrid is a group of energy sources, conventional and renewable. Moreover, it has to cater to different kinds of loads. A microgrid is a small-scale grid system that can work independently or in connection with the region's principal utility grid. Nowadays, the microgrid is the most popular entity since new renewable energy sources (RES) occasionally work better than connected to the utility grid. The RES that generally uses is solar PV due to the abundance of availability despite intermittency and matured PV cell technologies. Recently, more houses and facilities are catered by either utility-sized or rooftop solar power plant. [4].

For electrical energy generation, PV-module and wind power generators have become attractive options for renewable sources [5]. The wind-turbine based power generation is also considered an efficient system, moreover, these systems use comparatively less energy during manufacturing and also release less carbon dioxide under operation, and yet still generate more overall energy. Solar energy has an energy density of $1.5 \mu\text{J}/\text{m}^3$, while other inexhaustible such as wind and tidal have energy densities of 0.5 to $50 \text{ J}/\text{m}^3$ [6]. The wind-farms cannot be installed in highly populated areas and are harmful to birds [7]. So, solar PV based generation in a microgrid is sometimes preferred over wind-based generation. The solar PV cell converts sunlight directly into electrical energy and generates DC-voltage. Due to the variation in the irradiation level, the power generated from the PV module also varies with it. It is further beneficial to extract maximum possible power from the solar PV system, DC-DC converters with maximum power point tracking (MPPT) controller are employed together with PV inverters. The DC-DC boost converter assists in tracking the maximum power point and boosts the voltage to the required voltage level. The conventional power grid unification requires DC-AC converters which are also known as PV inverter along with controllers [8].

The PV based system offers many advantages, though it may suffer from uncertain environmental conditions and sudden changes in system loads. Moreover, for grid-tied PV systems, the probability of utility grid fault around the point of common coupling (PCC) might result in a system malfunction or the interference of power supplied to critical loads [9]. For uncertain disturbances, such as varying environmental conditions such as temperature and irradiation, fluctuating load demands, and occurrence of faults, cause the un-stabilized DC bus voltage, overshoot or undershoot, and sag or swell [10]. The aforementioned problems can be termed as the poor dynamics of PV control systems in differentiation to the transient time from the disturbances. In some cases, the requirements for fast dynamic compensation devices, like diesel generators or the BESS for power fluctuation management and mitigation of fault are effective alternatives [11]. The two major battery technologies used in EV are nickel-metal hydride (Ni-MH) and lithium-ion (Li-ion) [12]. The Ni-MH battery is a more popular choice but still expensive and needs technological development [13]. The Lead-acid type battery is presently the most preferred storage system

because matured technology offers reasonable cost and performance [11].

The EV charging in substantial proportion could raise various technical issues; including voltage regulation, variation in frequency harmonic distortion, etc. as a load on the power system. The fleet of EVs are considered as spinning reserves and their critical role as peak load shaving device; the associated issues in electrical network and challenges are discussed in [14]. The V2G concept has emerged to improve the performance of the electricity grid by addressing power quality issues such as management of active and reactive power, load balancing, and harmonic mitigation; and hence making the grid more stable and reliable [15,16]. The requirements of battery chargers and infrastructure needs for EVs are explained in [17]. An efficient energy management system gives a solution to manage EVs' charging load, which can help to minimize stress on the utility grid. The smart control techniques drew more attention to the impact of large-scale EVs carrying out V2G operations for energy management systems [18]. A simple battery scheme has been developed for the charging and discharging control of the EVs using a power electronic interface and the instantaneous power theory (p-q theory) based active filter to improve the PV system performance has also been analyzed for its effectiveness [19]. In this study, the various modes of operation of EV battery charging and uncertainty in load demand having PV as RES interfaced with electricity grid under microgrid scenario has been simulated and analyzed.

The paper is organized as follows: Section two discusses the modes of operation of the microgrid. Section three describes PV as a base source in the microgrid. Section four explains EV battery charging by the PV system mechanism. Section five includes EV battery charging through both solar PV systems and the grid. Section six describes V2G mode. Section seven concludes the outcomes of the work and the scope of future research work.

2. MODES OF OPERATION OF MICROGRID

The distribution of the power flow of the system is observed and controlled in four different modes. To route the power to flow in the given direction, critical steps are to determine the voltage magnitude next to the DC link (V_{DC}), the state of charge (SOC) of the EV battery (Lead-acid type), and the grid current (I_g). In different modes, the variation in solar power generation and the fluctuations in voltage level at the DC bus, the jurisdiction of the system is subjected to the observing and regulation of voltage levels at the PCC point [20]. The typical configuration of the IEEE 5-bus microgrid system consisting of a grid, different loads, PV, and EV is shown in Figure 1. The various modes of operation are as given below;

Mode I: PV operating as a base source in microgrid under balance condition

Mode II: EV charging through the PV system

Mode III: EV charging power demand fulfilled by both sources - solar PV and the utility power grid

Mode IV: Vehicle-to-grid (V2G) mode-the surplus energy in EV, and PV are fed into the grid simultaneously.

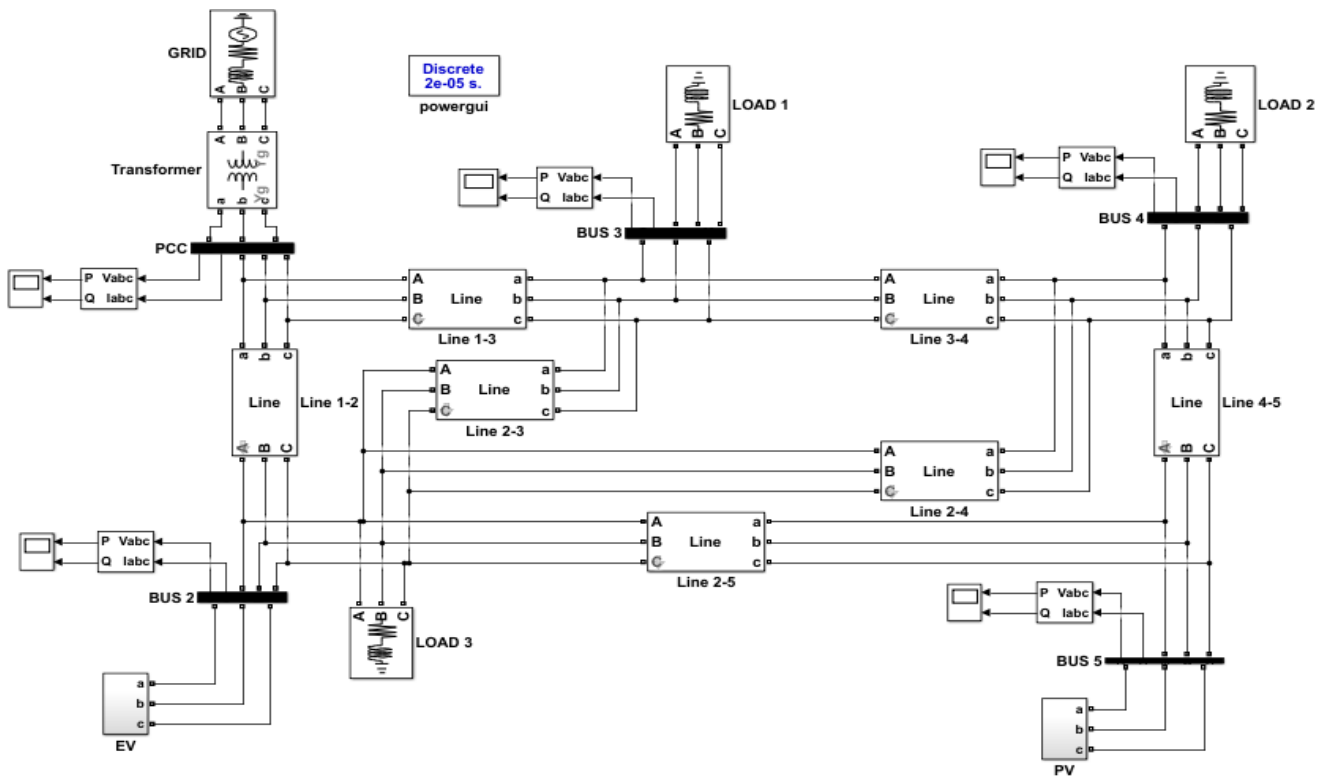


Fig. 1. IEEE 5 bus network system

3. PV AS A BASE SOURCE IN MICROGRID

The block diagram of the grid-tied PV system includes the solar PV panels, DC-DC boost converter, and inverter are shown in Figure 2. In this system, solar panel rating is considered to have 8 kW for the grid integration. The MPPT controller is used to take out the maximum power from the PV system due to its nonlinear characteristics. The Perturb and Observe (P&O) algorithm is one of the proven techniques.

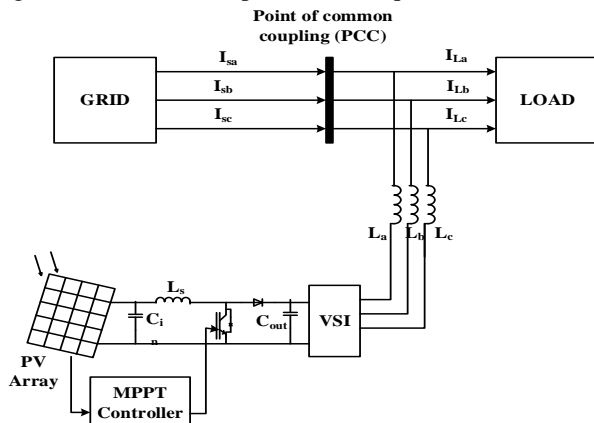


Fig. 2. Basic Block diagram of a grid-connected PV system

The boost converter is connected to the PV array and the three-phase VSI system uses six insulated gate bipolar transistor (IGBT) switches with anti-parallel diodes connected to the boost converter. The interfacing inductors (L_a, L_b, L_c) are used as a filter and help to reduce ripple in the compensating current. The inductor is connected at the point of common coupling (PCC) as an interfacing element [4].

The reference current estimation, load balancing, harmonics depletion, and power factor improvement is done by PV inverter using instantaneous symmetrical component theory (ISCT) control algorithm [21-22]. The block diagram of the ISCT algorithm [23] is as shown in Figure 3. The active power of the load can be calculated using the following equation:

$$P_1 = V_{sa} * I_{La} + V_{sb} * I_{Lb} + V_{sc} * I_{Lc} \tag{1}$$

where, V_{sa}, V_{sb}, V_{sc} are PCC voltages, and I_{La}, I_{Lb}, I_{Lc} are load currents respectively.

Reference current calculation can be done by using;

$$\begin{aligned} I_a^* &= [V_{sa} - (V_{sb} - V_{sc}) \beta] (P_{avg} + P_{loss}) / A \\ I_b^* &= [V_{sb} - (V_{sc} - V_{sa}) \beta] (P_{avg} + P_{loss}) / A \\ I_c^* &= [V_{sc} - (V_{sa} - V_{sb}) \beta] (P_{avg} + P_{loss}) / A \end{aligned} \tag{2}$$

where $A = \sum (V_{sa}^2 + V_{sb}^2 + V_{sc}^2)$ and $\beta = 0$ in the unity power factor control of grid-tied PV system. The generated reference currents from the calculation are then compared with actual source currents (I_a, I_b, I_c) using hysteresis current controller (HCC) that gives the results in the required six pulses for controlling PV inverter [4].

The PV system is modeled in MATLAB^(R)/Simulink. The system data is given in Appendix-1. The power generated by the solar PV system and utility grid meets the power required by the given load, and hence power balance is achieved. Moreover, the grid synchronization is possible by voltage, and frequency is assumed to be constant at the PCC point. The system parameters used in the simulation are listed in Table 1.

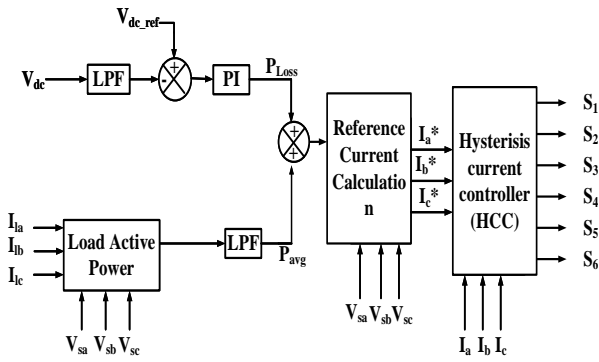


Fig. 3. The control scheme of PV inverter

Table 1. System parameters for Mode I

Sampling frequency	10 kHz
Series: Parallel connected PV panel	15: 2
Grid voltage	800 V
Load	20 kW, 5 kVAr

Figure 4 illustrates the waveforms of the voltage across PV (V_{pv}), current across PV (I_{pv}), grid voltage (V_{grid}), grid current (I_{grid}), load voltage (V_{load}), load current (I_{load}). Figure 5 shows the waveforms of PV power (P_{pv}), grid power (P_{grid}), load power (P_{load}). Figure 6 depicts the harmonic analysis for PCC current (I_{pcc}), and grid current (I_{grid}) and THD level is found to be 0.43% and 0.25%, respectively.

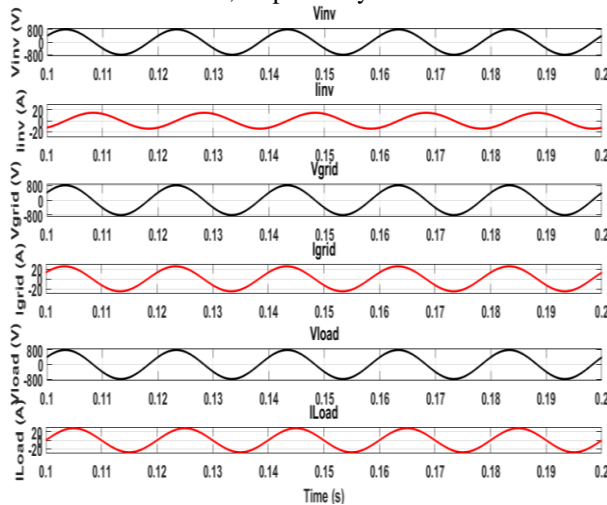


Fig. 4. Voltage and current waveforms of a grid-connected PV system

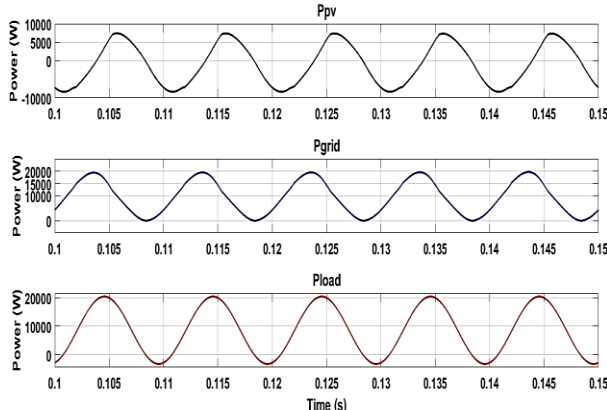
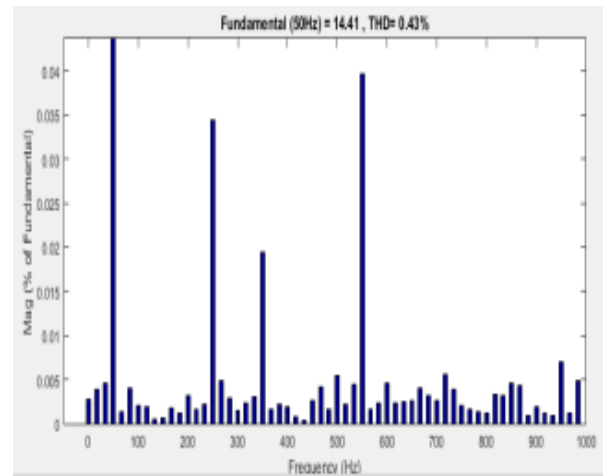
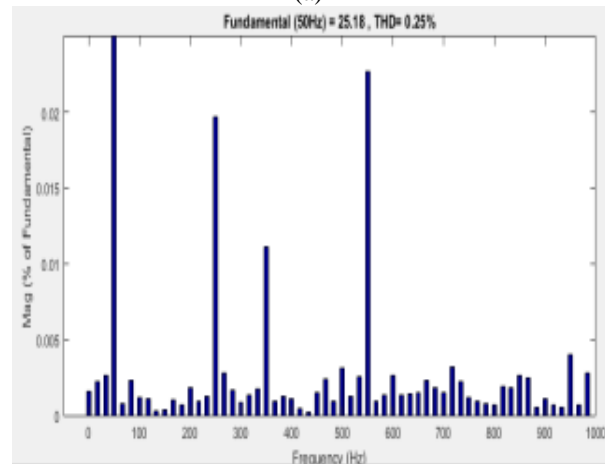


Fig. 5. Power transfer characteristic of a grid-connected PV system for linear load



(a)



(b)

Fig. 6. Harmonic analysis for PCC current (a) and grid current (b)

3.1 Performance of grid-connected PV system under varying irradiation levels

Figure 7 shows the variation in irradiation levels applied to simulation, assuming irradiation does not change abruptly but gradually. This pattern is given as an input to the PV module for observation of different irradiation cases. Up to 0.6 s, the irradiation level is assumed to be 500 W/m², 0.8 s to 1.2 s, 800 W/m², 1.4 s to 1.6 s, 600 W/m², and 1.8s to 2.2s, the irradiation level is 1000 W/m². This confirms the variation in solar irradiation level in the real situation.

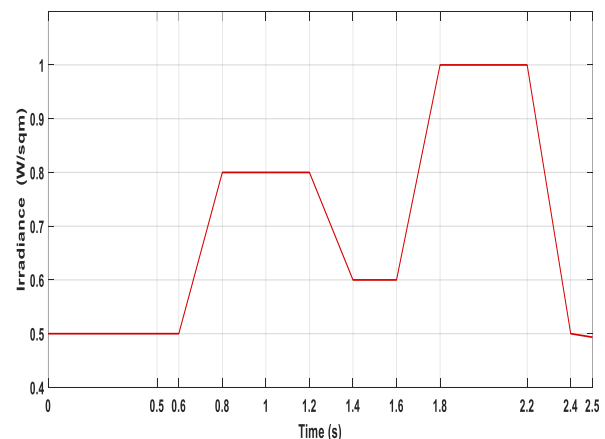


Fig. 7. Characteristic of varying irradiation levels

Figure 8 shows the tracking of the MPP of the PV system with varying irradiation levels. The waveforms of voltage across PV (V_{pv}), current across PV (I_{pv}), power across PV (P_{pv}) is shown in Figure 9. The value of power is changed with the change in the irradiation level. In figure 10 power transfer characteristic is shown, in which the output power of PV and power of the grid is combined to fulfill the load power demand which is achieved at a unity power factor. Figure 11 shows the harmonic analysis for PCC current (I_{pcc}), grid current (I_{grid}), and THD levels are observed to be 6.36% and 5.27%, respectively.

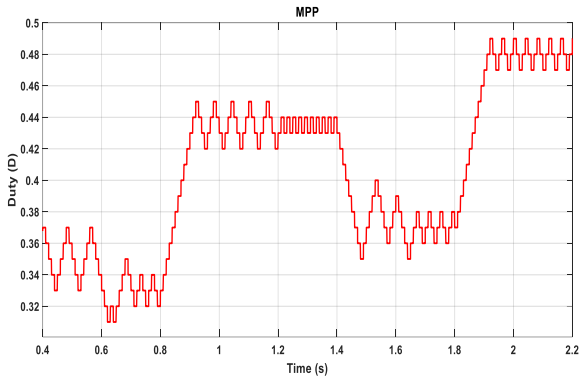


Fig. 8. MPPT under varying irradiation levels

3.2 Performance of grid-connected PV system under different load conditions

The grid-connected PV system is connected with three different types of loads. One is purely active load is connected to the system up to 1.5 s of total time. A more practical kind of load that draws active and reactive as well is connected to the system between 1.5 s to 2 s of total time. The third kind of load predominantly active load and partial reactive load which is connected to the system. The breaker is used to control the load operation. The system parameter used for simulation is given in Table 2.

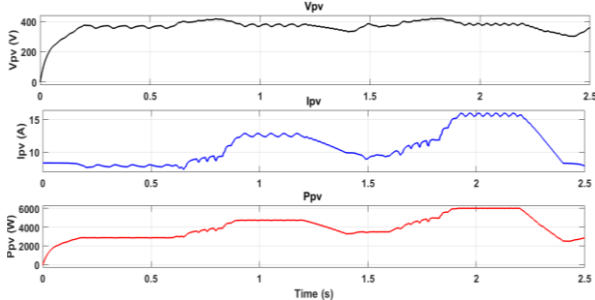


Fig. 9. The waveform of the grid-connected PV system for varying irradiation level

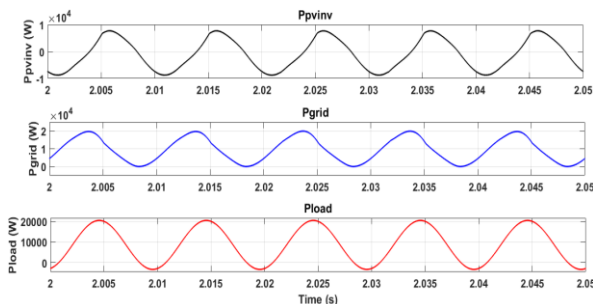
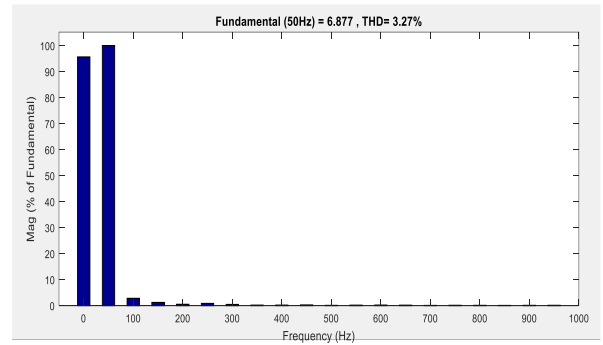
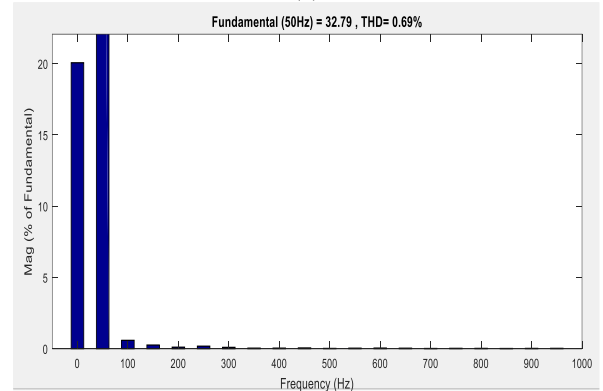


Fig. 10. Power transfer characteristic of the PV system for varying irradiation level



(a)



(b)

Fig. 11. Harmonic analysis of PCC current (a), and grid current (b)

Table 2. System parameter for various load condition

Load Condition	System Parameter
Pure active load	20 kW
Active and reactive load	20 kW, 5 kVar
Major active load	14 kW, 1.5 kVar

The waveforms of PV inverter voltage (V_{inv}), current (I_{inv}), power (P_{inv}) are shown in Figure 12. The value of power is changed by varying the load connected. In Figure 13, the power transfer characteristic is illustrated, in which the power from PV and grid are combined to meet the load power, and is at unity power factor. When the active load is connected to the system, the fluctuation is very less, and by connecting active and reactive load, the fluctuation level becomes dominating as shown in Figure 13. The harmonic analysis is shown in figure 14 for PCC current (I_{pcc}) and grid current (I_{grid}). THD level is 2.10% and 1.51% respectively.

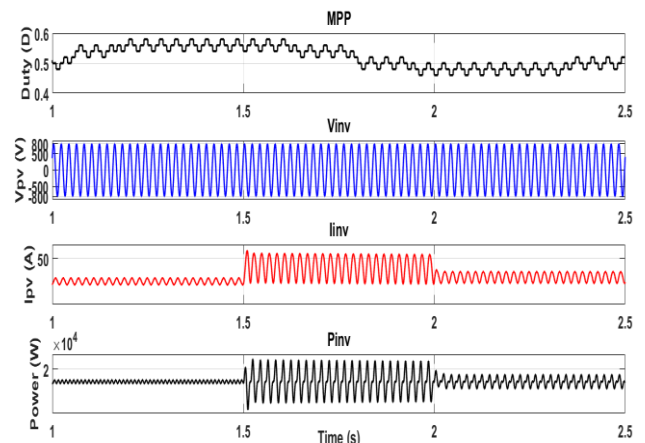


Fig. 12. Performance of grid-connected PV system under different load conditions, a) duty ratio, b) inverter voltage, c) inverter current and, d) inverter output power

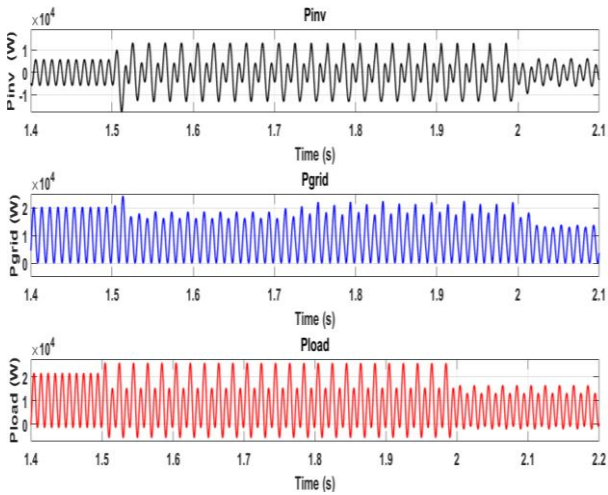
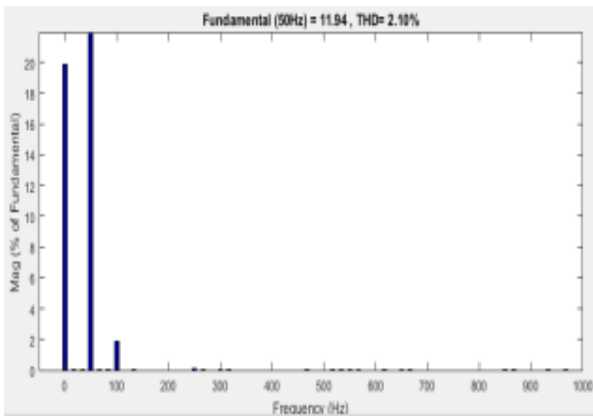
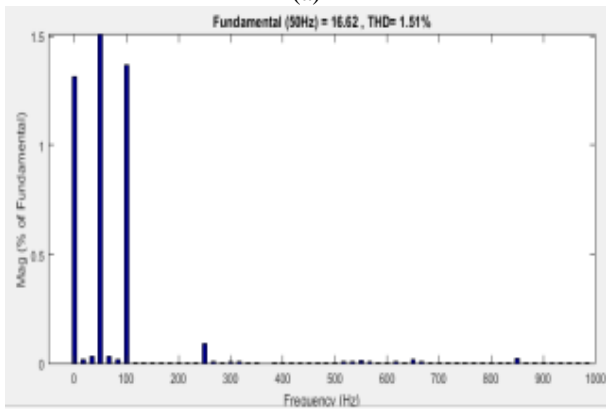


Fig. 13 Power transfer under different load conditions, a) inverter output power, b) power from the grid, c) load power demand



(a)



(b)

Fig. 14. Harmonic analysis of (a) PCC current and (b) grid current

4. EV BATTERY CHARGING BY PV SYSTEM

Figure 15 shows Mode II operation, in which all the solar energy is used for charging batteries of EVs initially, and the DC bus voltage is maintained close to 500 V. If solar energy continues to grow or EV charging demand is satisfied, then the surplus power is fed into the utility grid. In this respect, it can be seen that firstly, the whole EV charging is being supported by PV power generation only, as an adequate amount of solar energy is accessible [18]. The system parameter for simulation is given in Table 3.

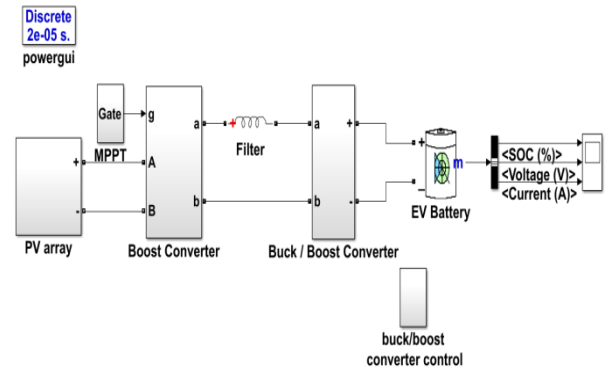


Fig. 15 Simulink model of EV battery charging by a PV system

Table 3. System parameter for mode II

Battery type	Lead-acid
Battery nominal voltage	240 V
Rated capacity	3 Ah
Initial SOC	20 %

Figures from 16 to 21 show waveforms for mode II. In Figure 16, the status of SOC of the EV battery, charging is shown. Figure 17 shows the MPP waveform that is tracked by three points. Figure 18 includes the DC bus voltage that is maintained to be constant at 265 V. The PV system output is given in Figure 19 illustrating V_{pv} , I_{pv} , and P_{pv} . In this case, the power flows from PV to battery and load. The waveforms of PV power (P_{pv}), battery ($P_{battery}$), and load power (P_{load}) are given in Figure 20. The THD of PV current is 5.24% as shown in Figure 21.

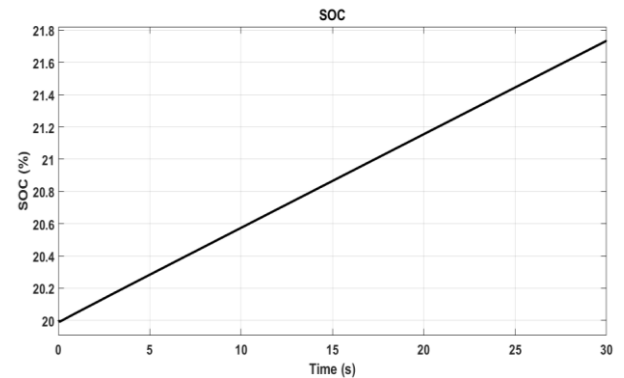


Fig. 16. SOC increase under Mode II operation

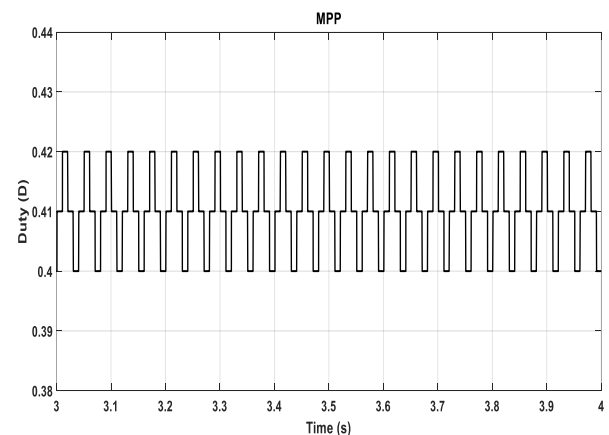


Fig. 17. Tracking of MPP under Mode II operation

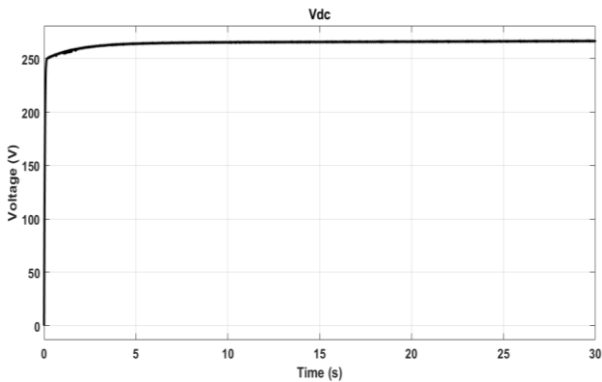


Fig. 18. DC Bus Voltage under Mode II operation

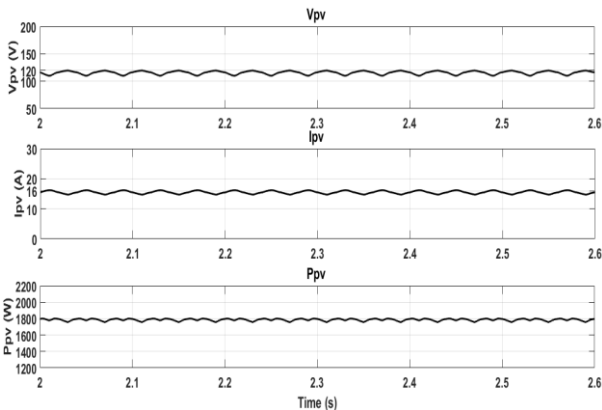


Fig. 19. Performance of PV system under Mode II operation (PV voltage, PV current, and PV power)

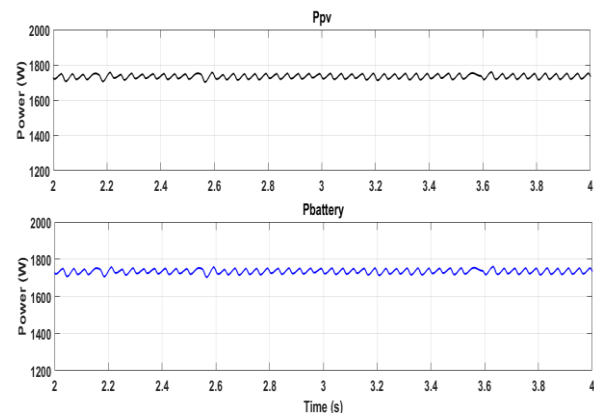


Fig. 20. Power transfer characteristic under Mode II operation

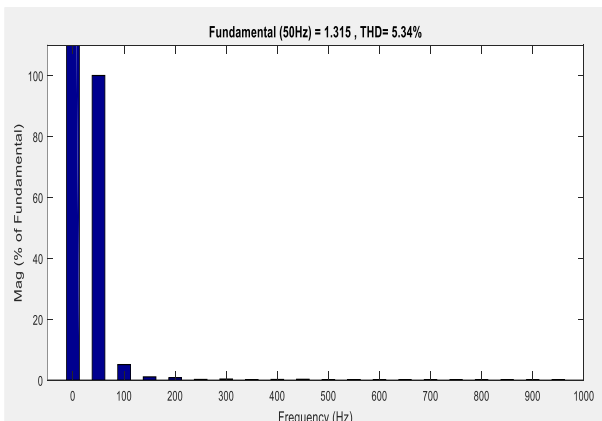


Fig. 21. Harmonic analysis of PV output current under Mode II operation

5. EV BATTERY CHARGING BY PV SYSTEM AND GRID

Under Mode III, the corresponding power from the PV system is not sufficient to meet the EV charging power request, and thus, it has to be supplied through both sources, i.e. the PV system and the utility grid. Then EV charging power demand is being reached by both PV and the utility power grid [18].

The layout of the considered single-stage grid-connected PV and BES system is as shown in Figure 22. The system contains a PV generator that is connected to the DC bus through a DC/DC buck converter with an MPPT controlling technique. The inverter simplifies the MPPT operation through adjustment of the DC bus voltage as well as it conveys power from the DC bus to the utility grid. Also, the inverter is equipped with synchronization of the PV system with the grid during start-up or reunification after system islanding.

As can be seen from Figure 22, to improve the DC bus voltage regulation, BES is used where it is coherence via a bidirectional buck-boost converter (BES converter). The role of this is to control the charge or discharge processes during different operating conditions such as a radical change in solar irradiation level and fault occurrence. An inverter is coupled with the utility grid at PCC through an interconnecting transformer which is also acting as a low-pass filter. The low pass filter is accountable for filtering harmonics and isolating the whole system from the utility grid. The step-up transformer is used to increase the voltage level of the PV system from 230 V to 11 kV line-to-line RMS voltage. The PV/BES system supplies its total power to the utility grid in which this case the utility grid network is based on a standard medium voltage distribution system [24].

The control of the charging/discharging of BES is achieved by using a buck-boost converter comprising two PI controllers, as shown in Figure 23. The first PI gives an error in the DC bus voltage by comparing actual regarding the bus voltage $V_{DC, ref} = 500$ V. The second PI controller takes care in ensuring the compensated battery current. The output signal given by the second PI is passed to the pulse-width-modulator (PWM) generation circuit where the logical circuit is used for the decisions to make like the charge, discharge, or halt modes of operation [11].

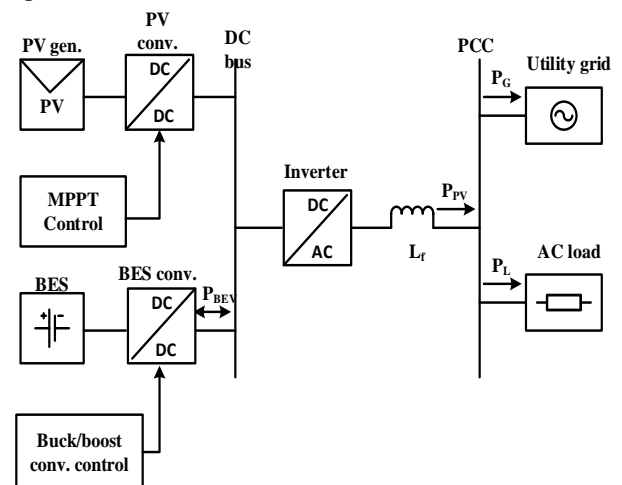


Fig. 22. The system configuration of grid-connected PV with EV

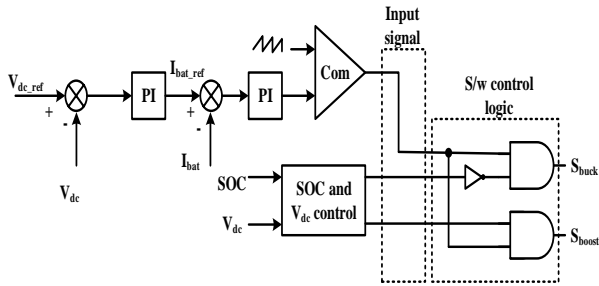


Fig. 23. The buck-boost converter control scheme

Figure 24 shows the algorithm developed for SOC and bus voltage control to make sure a reliable and optimal operation of BES. The upper and lower limits of SOC denoted as SOC_H and SOC_L are defined to avoid overcharge or deep discharge of BES. As a result, the upper and lower boundaries of the DC bus voltage control are also contemplated to avoid unnecessary charging/discharging. In this case, the battery is set to charge/discharge only when the departure of DC bus voltage exceeds a certain range denoted as $V_{DC,H}$ and $V_{DC,L}$, respectively. The algorithm utilizes the inputs the SOC and the DC bus voltage where the output from this algorithm provides input for the control logic circuit for determining the correct operating modes [11] which are shown in Figure 23.

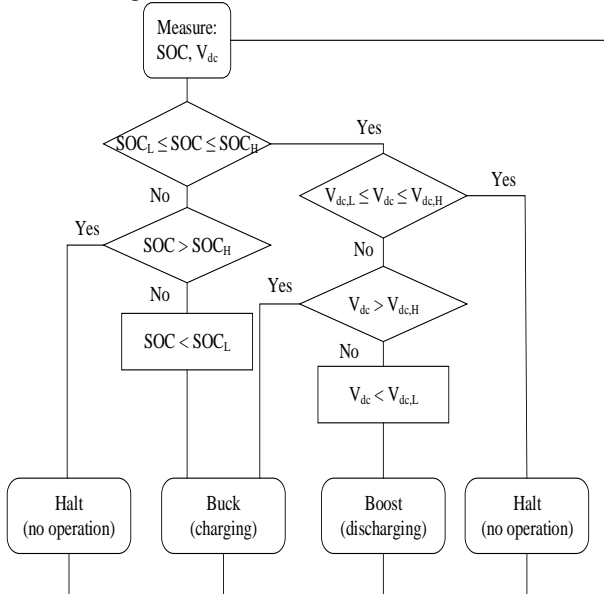


Fig. 24. Flowchart of SOC and EV power charge/discharge control

The buck-boost converter control algorithm is set to operate between the SOC limit of 50% and 80%. If the SOC level drops below 50% then the battery should in charging mode, and if the battery SOC level drops below 80% then the battery should be discharged. In Mode III operation, the value of the lower value of DC bus voltage is set as 750 V and the upper limit as 850 V.

The system parameter for simulation is given in Table 4.

Table 4. System parameter for Mode III

Grid voltage	800 V
Load	20 kW, 5 kVar
Battery type	Lead-acid
Initial SOC	48 %

Figures 25, 26, 27, 28, and 29 show waveforms of mode III. In figure 25, the SOC of the EV battery is given. The battery is charging by both PV and grid, so the battery charging is faster compared to Mode II. After crossing SOC value 50%, the battery should stop charging, and SOC remains constant. Figure 26 shows the MPP waveform that is tracking by a three-point method ensuring MPPT operation. Figure 27 indicates the DC bus voltage which is constant at 710 V. After crossing SOC 50%, the DC bus voltage increase to 800 V and then remain constant. The waveform shows the voltage value of 710 V that is the same as the DC bus voltage.

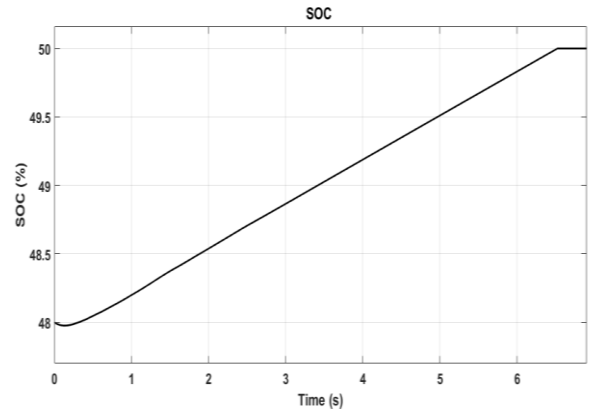


Fig. 25. SOC increase under Mode III operation

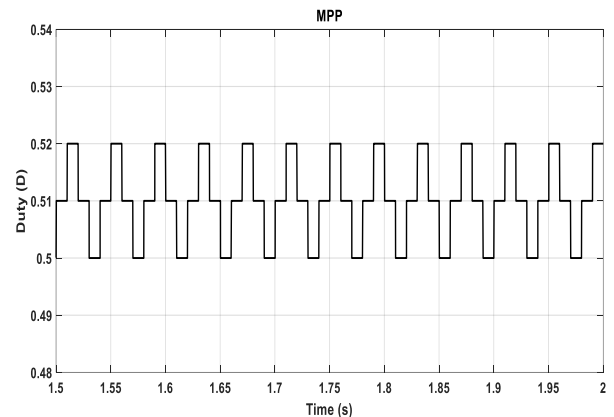


Fig. 26. Tracking of MPP under Mode III operation

All these waveforms are having distortions, so we use an LC filter to reduce distortion. In this case, the power flows from PV and grid to a battery. The waveform of PV inverter power (P_{pvinv}), grid power (P_{grid}), battery power ($P_{battery}$), load power (P_{load}) are shown in Figure 28.

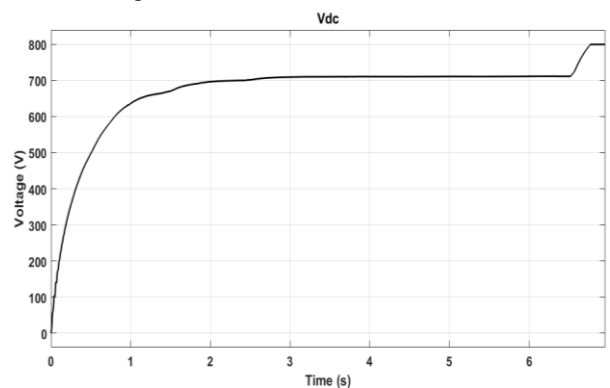


Fig. 27. DC bus voltage under Mode III operation

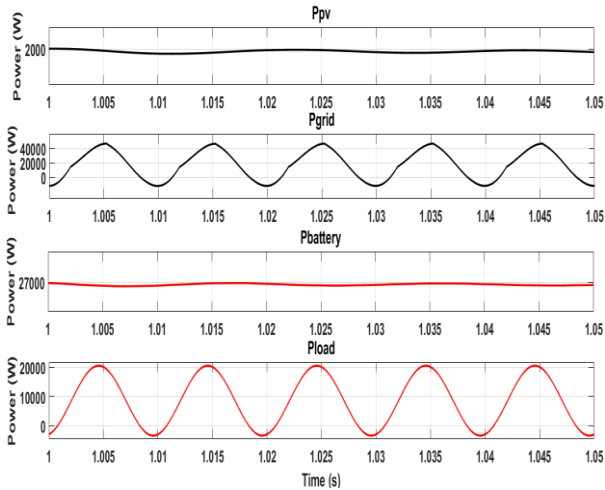


Fig. 28. The waveform of power transfer from PV and grid to battery and load

Figure 29 shows the harmonic analysis for grid current (I_{grid}), PV inverter current (I_{inv}), and EV battery current ($I_{battery}$) respectively. THD for grid current is 2.90% THD for PV inverter current is 3.86%, and THD for EV battery current is observed to be 4.57%.

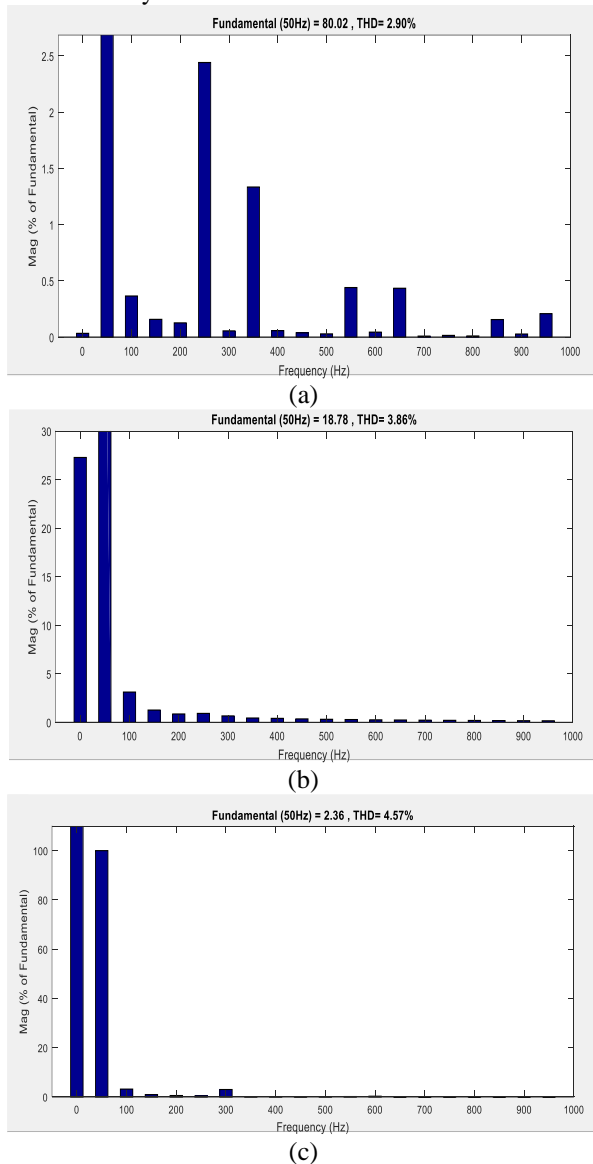


Fig. 29. Harmonic analysis of grid current (a), PV inverter current (b), and EV battery current (c) under Mode II operation

6. VEHICLE-TO-GRID (V2G) MODE

The V2G strategy proposes a system, in which different EVs communicate with the utility grid to offer services by feeding electricity to the grid or by managing the charging rate of EVs. Since most of the EVs are parked 95% of the time [25], their batteries can be useful for letting electricity flow between the vehicles and the grid. The EV batteries can occupy or purchase electrical energy from the grid during the off-peak period called load leveling in the V2G concept, but produce or vend electrical energy to the grid during the peak period called load shaving [26].

In the studied configuration, the bi-directional PWM power converter deals with power swapping between the grid and the EV battery charger. Smart chargers are designed such that they either supply power from PV and/or grid or feeds power from EV into the grid during peak load hours [18].

The V2G mode analysis has been carried out for the IEEE 5 bus system as shown in Figure 1. This microgrid consists of a utility grid, PV system, EV battery, and three different loads. The grid source is assumed to 100 MVA and 22 kV and connected through a transformer of 22KV/400V. The PV, EV battery, and other loads are connected to the grid through the PCC. The value of the load is increasing suddenly and the grid does not have a sufficient amount of energy to fulfill the load demand. In this condition, the EV battery is getting ready to transfer its energy back to the grid. The PV system is also working at the MPP level and transfer energy to the grid to compensate for the load.

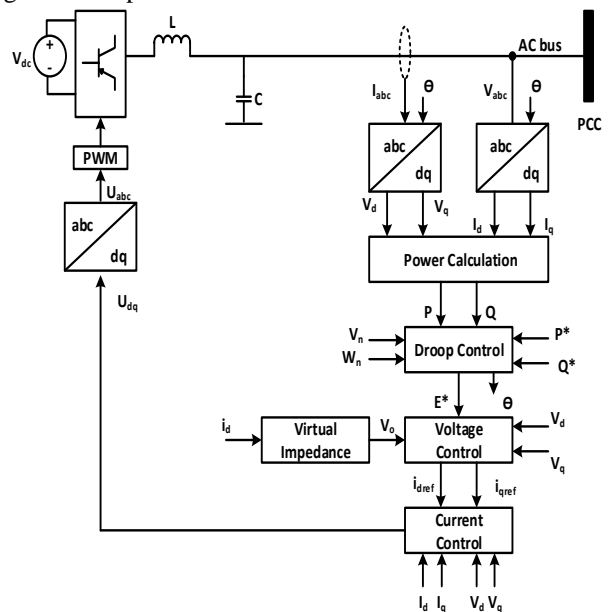


Fig. 30. The control scheme of the inverter by droop voltage control method

Since, PV and EV being DC source, to convert from DC to AC, inverter control by droop voltage control method is engaged. The droop voltage control method circuit diagram [27] is shown in Figure 30. In figure power calculation [28] block, droop control [29], voltage control [30], virtual impedance [31] and current control [32] block is employed. The droop voltage control method is being adopted for analysis to make the system flexible and expandable and is explained below.

Power Calculation:

$$P = \frac{3}{2} * (V_d * i_d + V_q * i_q)$$

$$Q = \frac{3}{2} * (V_q * i_d - V_d * i_q) \quad (3)$$

Droop Control:

$$E^* = V_n - K_p (P^* - P) \quad (4)$$

$$W^* = W_n - K_q (Q^* - Q) \quad (5)$$

$$\text{And } \Theta = \int W^*$$

where, $K_p = \frac{\Delta(W)_{\max}}{P_{\max}}$ and $K_q = \frac{\Delta(V)_{\max}}{Q_{\max}}$

Virtual Impedance:

$$V_o = i_d * R_D \quad (6)$$

Voltage Control:

$$V_{\text{ref}} = E^* - V_o$$

$$i_{d\text{ref}} = [K_p + \frac{K_i}{s}] (V_{\text{ref}} - V_d)$$

$$i_{q\text{ref}} = [K_p + \frac{K_i}{s}] (-V_q - V_o) \quad (7)$$

Current Control:

$$U_d = V_d + R i_d + L \frac{di_d}{dt} - \omega L i_q$$

$$U_q = V_q + R i_q + L \frac{di_q}{dt} - \omega L i_d \quad (8)$$

The system parameter for simulation is given in Table 5.

Table 5. System parameter for Mode IV

Grid voltage	22 kV
Transformer	22/0.4 kV
Battery type	Lead-acid
Initial SOC	82 %
Load 1	400 V, 50 kW, 35 kVar
Load 2	400 V, 50 kW, 35 kVar
Load 3	400 V, 50 kW, 35 kVar

The relevant waveforms for mode IV are depicted in Figures 31-34. In figure 31, the SOC of the EV battery is illustrated. The battery is getting discharged to the grid as the grid not having sufficient, and the battery having the energy to transfer as the SOC level is 82%. The battery is discharging up to SOC level 80% only. After the SOC value 80% the battery is in no transfer condition. So we can say that the EV battery is in discharging mode.

Figure 32(a) shows the MPP waveform that is tracking by a three-point method. The PV is transferring energy to the grid. Figure 32(b) includes the DC bus voltage across the EV battery, which is constant at 500 V. Figure 32(c) shows the DC bus voltage across the PV system. All these waveforms are having distortions; an LC filter is used to reduce the level of distortion. In this case, the power flows from PV and battery to load. The waveform of PV grid power (P_{grid}), inverter power (P_{pvinv}), battery power ($P_{battery}$), load power (P_{load}) of three different loads is given in Figure 33. After transferring the power from PV and battery, the grid source has a sufficient amount of energy to transfer to the load.

Figure 34 shows the Harmonic analysis for grid current (I_{grid}), PV inverter Current (I_{inv}), and EV battery current ($I_{battery}$) respectively. THD for Grid current is 0.09% THD for PV inverter current is 3.36%. THD for EV battery current is 0.37%. The THD is also improved compared to Mode III.

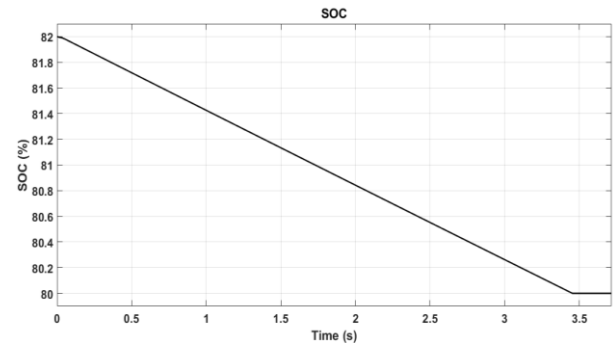
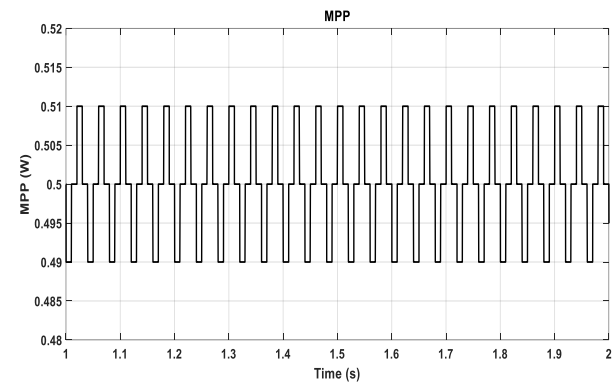
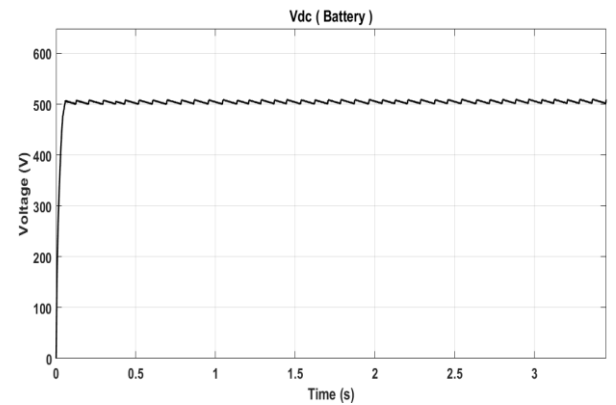


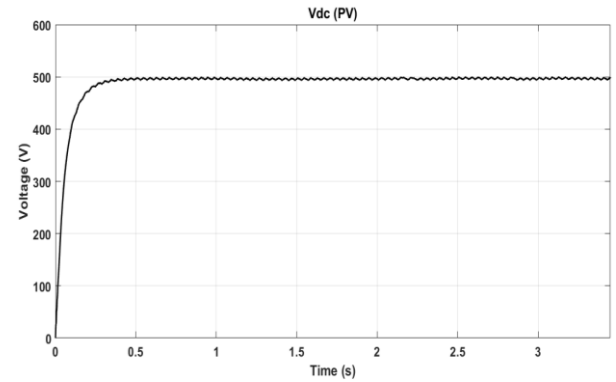
Fig. 31. SOC decrease under Mode IV operation



a)



b)



c)

Fig. 32. a) Tracking of MPP of PV system, b) DC bus-voltage across EV Battery, c) DC bus-voltage across PV system

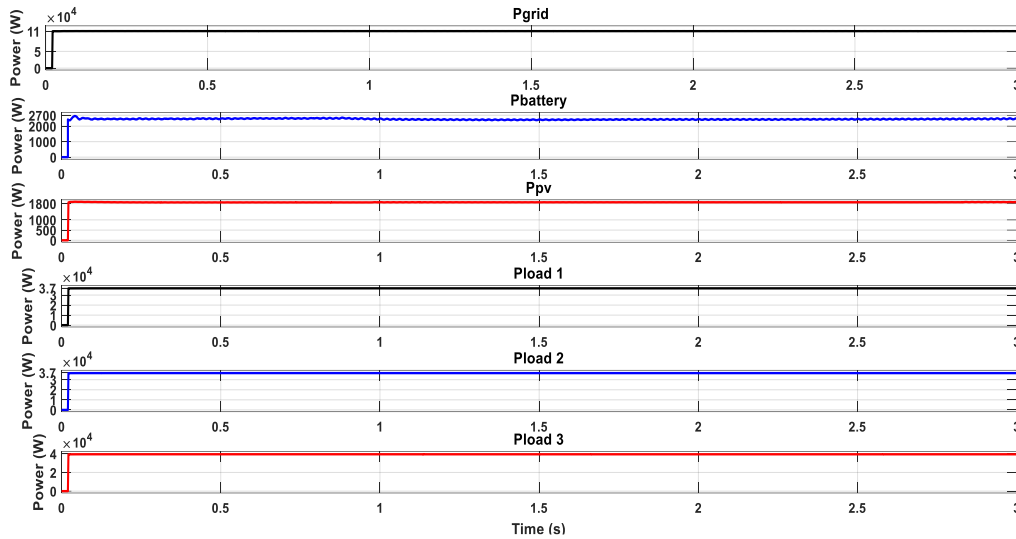


Fig. 33. Power transfer from PV and battery to grid

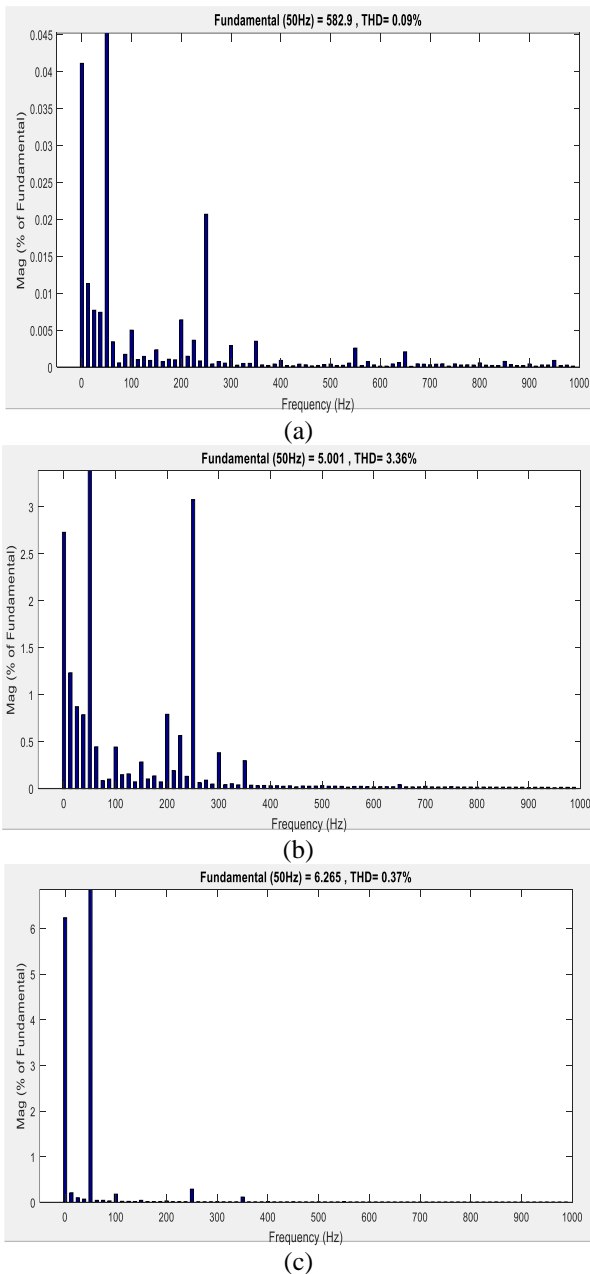


Fig. 34. Harmonic analysis of grid current (a), PV inverter current (b), and EV battery current (c) under Mode IV operation

7. CONCLUSIONS

From this analysis, it is clear that not only the stability of the utility grid is improved but also, some other economic benefits could be achieved by incorporating the V2G concept in the microgrid. The distribution of power was monitored and controlled in four different kinds of modes. The first mode includes the simulation studies on the PV system connected to the utility grid. This study was performed under different load and irradiation conditions. Under all these conditions, the DC link voltage was maintained within a narrow range, and hence, the power balance was also ensured undercharging of the EV and V2G operation. The power factor of the grid injected current was also maintained to be unity with the help of the d-q theory. In mode II, the EV battery was charged through the PV system, though the charging process seems a little sluggish. The DC bus voltage is maintained constant. In mode III, the PV source was not able to fulfill the energy demand of the battery so the grid was also connected to the system to support it. In this case, the buck/boost converter is employed for energy management through controlling SOC and DC bus voltage. In mode IV, a microgrid having IEEE 5 bus system was analysed. For V2G mode, inverter control by droop voltage control method is analysed. During peak load conditions, an EV with surplus power was pumped into the grid and was governed by a control algorithm. To harness the optimum power, the PV system was forced to operate at MPP. With this V2G concept, it has been inferred that without investing in additional storage the electric vehicles' batteries themselves act as a source of energy storage.

As possible future work, the system could be simulated under more variable climatic conditions, like temperature, along with different irradiation levels. A similar analysis could be carried out with other sources of energy, like wind, bio/diesel generator, etc. to study more realistic microgrid systems as well. The design of a more intelligent energy/power management system would be another research aspect.

Appendix-I

P, Q : Real active and reactive power
P^*, Q^* : Nominal value active and reactive power
ω_n, V_n : Nominal rate of angular frequency (rad/sec) and voltage amplitude (v)
K_p, K_q : The droop coefficients related to active and reactive power
$\Delta(\omega)_{max}, \Delta(V)_{max}$: The maximum angular frequency and voltage deviations
P_{max}, Q_{max} : The maximum real and reactive power delivered by the power converter.
V_o : Voltage fall across a virtual impedance
I_d : The inverter output current
R_D : The virtual impedance (resistor)
E^* : Voltage reference signal
V_{ref} : Modified voltage reference signal
$I_{dref} - I_{qref}$: d-axis and q-axis reference current component
$U_d - U_q$: The output voltage signal in the d-q form
ω : Angular frequency
L : Inductance between inverter and PCC network [18]

Appendix-II

Details of the solar PV system
Rated power (P_{max}) = 8 kW
PV module specifications (at STC*)
Voltage at maximum power (V_{mpp}) = 36 V
Current at maximum power (I_{mpp}) = 7.78 A
Open circuit voltage (V_{oc}) = 44.6 V
Short circuit current (I_{sc}) = 8.32 A
*STC (Standard Test Cond.): Irradiance 1000 W/m ²
Cell temperature 25 °C, AM 1.5
DC-DC boost converter
D=0.5
L=0.0005 H
C=1000 μ F
PV inverter
V_d =800 V
$L_{inverter}$ =10 mH
C_d =1000 μ F

Acknowledgment

The authors would like to express special thanks of gratitude to Sarvajanic College of Engineering & Technology, Surat for providing facilities to carry out this research, and also expert reviewers for their valuable suggestions to shape this manuscript more informative. This research received no external funding. The authors declare no conflict of interest.

References

[1] F. Mwasilu, J. J. Justo, E-K. Kim, T. D. Do, J-W. Jung, Electric vehicles, and smart grid interaction: A review on a vehicle to grid and renewable energy sources integration, *Renewable and Sustainable Energy Reviews*, 34, 501-516, (2014).

[2] M. Aziz, T. Oda, T. Mitani, Y. Watanabe, and T. Kashiwagi, Utilization of Electric Vehicles and Their Used Batteries for Peak-Load Shifting, *Energies*, 8(5), 1-19, (2015)

[3] O. I. Aloqaily, I. Al-Anbagi, D. Said and H. T. Mouftah, Flexible charging and discharging

algorithm for electric vehicles in smart grid environment, *IEEE Wireless Communications and Networking Conference*, Doha, 1-6, (2016).

[4] M. Kumar, N. Gupta, and R. Garg, Unity Power Factor Control of Grid Connected SPV system using Instantaneous Symmetrical Component Theory, 2016 IEEE 1st International Conference on Power Electronics, Intelligent Control and Energy Systems (ICPEICES), Delhi, 1-6, (2016).

[5] N. Gupta, R. Garg, and P. Kumar, Characterization study of PV module connected to microgrid, *Annual IEEE India Conference (INDICON)*, New Delhi, 1-6, (2015).

[6] B. E. Layton, A Comparison of Energy Densities of Prevalent Energy Sources in Units of Joules Per Cubic Meter, *International Journal of Green Energy*, Taylor & Francis Group, 5, 438-455, (2008).

[7] R. Alessandra, An In-depth Comparison: Solar Power vs. Wind Power, *Knowledge Base*, (2019).

[8] A. El-Shahat and S. Sumaiya, DC-Microgrid System Design, Control, and Analysis, *Electronics*, 8(124), (2019).

[9] A. Nabil. A. Ahmed, K. Al-Othman, and M. R. Alrashidi, Development of an efficient utility-interactive combined wind/photovoltaic/fuel cell power system with MPPT and DC bus voltage regulation, *Electric Power Systems Research*, 81, 1096-1106, (2011).

[10] A. Hajizadeh, M. A. Golkar, Control of hybrid fuel cell/energy storage distributed generation system against voltage sag, *International Journal of Electrical Power and Energy Systems*, 32, 488-497, (2010).

[11] M. Z. Daud, A. Mohamed, and M. A. Hannan, An optimal control strategy for DC bus voltage regulation in photovoltaic system with battery energy storage, *The Scientific World Journal*, (2014).

[12] K. Young, W. Caisheng, W. Le, K. Strunz, *Electric Vehicle Battery Technologies Electric Vehicle Integration into Modern Power Networks*, 15-56, (2013).

[13] Alternative Fuels Data Center, https://afdc.energy.gov/vehicles/electric_batteries.html, U.S. Department of Energy, [Online]. Available: <http://www.eere.energy.gov>. [Accessed on June 2020].

[14] C. Tsoleridis, P. Chatzimisios, and P. Fouliras, Vehicle-to-Grid Networks: Issues and Challenges, Chapter 14, in *Smart Grid*, Taylor & Francis Group, pp. 347-366, (2016)

[15] M. Yilmaz, and P. T. Krein, Review of benefits and challenges of vehicle-to-grid technology, *IEEE Energy Conversion Congress and Exposition (ECCE)*, Raleigh, NC, 3082-3089, September, (2012).

[16] M. Yilmaz and P. T. Krein, Review of the Impact of Vehicle-to-Grid Technologies on Distribution Systems and Utility Interfaces, *IEEE Transactions on Power Electronics*, 28(12), 5673-5689, (2013).

[17] M. Yilmaz, and P. T. Krein, Review of Battery Charger Topologies, Charging Power Levels, and Infrastructure for Plug-In Electric and Hybrid

- Vehicles, in IEEE Transactions on Power Electronics, 28(5), 2151-2169, (2013)
- [18] A. Ul-Haq, C. Cecati, and A. Al-Ammar, Modelling of a Photovoltaic-Powered Electric Vehicle Charging Station with Vehicle-to-Grid Implementation, Energies, 10(4), (2017).
- [19] F. R. Islam and H. R. Pota, Design a PV-AF system using V2G technology to improve power quality, IECON 2011 - 37th Annual Conference of the IEEE Industrial Electronics Society, Melbourne, VIC, 861-866, (2011).
- [20] M. E. Şahin, A photovoltaic powered electrolysis converter system with maximum power point tracking control, International Journal of Hydrogen Energy, 45, (2020).
- [21] A. Ghosh, and A. Joshi, A new approach to load balancing and power factor correction in power distribution system, IEEE Trans. Power Delivery, 15(5), 417-422, (2000).
- [22] A. Ghosh, and G. Ledwich, Load Compensating OSTATCOM in Weak AC Systems, IEEE Trans. Power Delivery, 18(4), 1302-1309, (2003).
- [23] S. Kumar, and B. Singh, Control of 4-Leg VSC Based OST ATCOM using Modified Instantaneous Symmetrical Component Theory, Third international conference on Power System, ICPS, India, (2009).
- [24] K. Strunz, E. Abbasi, R. Fletcher, N. Hatziargyriou, R. Iravani, G. Joos, TF C6.04.02: TB 575 -- Benchmark Systems for Network Integration of Renewable and Distributed Energy Resources, (2014).
- [25] IRENA, Innovation outlook: Smart charging for electric vehicles, International Renewable Energy Agency, Abu Dhabi, (2019).
- [26] R. Folkson, Alternative Fuels and Advanced Vehicle Technologies for Improved Environmental Performance, 1st Edition Woodhead Publishing, (2014).
- [27] A. Vinayagam, KSV. Swarna, Y. S. Khoo, O. Yong, Aman, A. Stojcevski, PV Based Microgrid with Grid-Support Grid-Forming Inverter Control- (Simulation and Analysis), Smart Grid and Renewable Energy-Scientific Research Publishing, 8, 1-30, (2016).
- [28] M. Khederzadeh, H. Maleki, Frequency Control of Microgrids in Autonomous Mode by a Novel Control Scheme Based on Droop Characteristics, Electric Power Components and Systems, 16, 16-30, (2013).
- [29] J. M. Guerrero, L.G. Vicuna, J. Matas, M. Castilla, and J. Miret, Output Impedance Design of Parallel-Connected Ups Inverters with Wireless Load-Sharing Control, IEEE Transactions on Industrial Electronics, 52, 1126-1135, (2005).
- [30] Z. Jiang, X. Yu, Active Power-Voltage Control Scheme for Islanding Operation of Inverter-Interfaced Microgrids, IEEE Power & Energy Society General Meeting, Calgary, 1-7, (2009).
- [31] H. Han, X. Hou, J. Yang, J. Wu, M. Su, and J. M. Guerrero, Review of Power Sharing Control Strategies for Islanding Operation of AC Microgrids, IEEE Transactions on Smart Grid, 7, 200-215, (2016).
- [32] A. Vargas-Serrano, D. Saez, L. Reyes, B. Severino, R. Palma-Behnke, and R. Cárdenas-Dobson, Design and Experimental Validation of a Dual Mode VSI Control System for a Micro-Grid with Multiple Generators, IECON 2012 38th Annual Conference on IEEE Industrial Electronics Society, Montreal, 5631-5636, (2012).

Biographies



Zeel Antrixkumar Padhya graduated in Electrical Engineering from Uka Tarsadia University, Surat, Gujarat, in 2018 and completed M.Sc. in Electrical Engineering from Sarvajanik College of Engineering & Technology, affiliated with Gujarat Technological University, Ahmedabad, India. Currently, she is working in the R&D department of Tech Sun Bio Pvt. Ltd. Surat, India. Her area of interest includes grid integrated renewable energy sources, electrical vehicles, design, and modeling of power electronics converter.
E-mail: zpadhya@gmail.com



Shabbir Saleh Bohra has been working as a Professor in the Electrical Engineering Department, Sarvajanik College of Engineering & Technology (SCET), Surat (Guj), India. He was a guest researcher in the Department of Energy Technology at Aalborg University, Aalborg, Denmark. He is a Government of India certified energy auditor. His research interests are renewable energy sources, energy management, grid-interactive PV System, hybrid micro-grid, and power quality. He received his bachelor's degree in Electrical Engineering from S. V. National Institute of Technology, Surat, India in 1999 and his Master's degree in Energy Systems Engineering from Indian Institute of Technology (IIT)-Mumbai, India in 2007. He was awarded Ph.D. in Modelling of Advanced Si-Solar Cells from S. V. National Institute of Technology (SVNIT), Surat, India in 2015. He has authored and co-authored several technical research papers in peer-reviewed national and internationally renowned conferences and journals and has been associated with many solar photovoltaic and energy management projects.
E-mail: bohra.shabbir@gmail.com